Ion Binding by X-537A. Formulas, Formation Constants, and Spectra of Complexes†

Hadassa Degani* and Harold L. Friedman

ABSTRACT: Circular dichroism and fluorescence spectroscopy have been applied to determine the stoichiometries and formation constants (selectivities) of the complexes of the carboxylic antibiotic X-537A (XH) with Li^+, Na^+, K^+, Rb^+, Cs^+, Mg^{2+}, Ca^{2+}, Sr^{2+}, Ba^{2+}, Mn^{2+}, and Ni^{2+} in methanol and *n*-hexane taking into account the $XH \rightarrow X^- + H^+$ dissociation. In methanol the complexes mostly have the formulas MX or MX^+ but species MHX^+ also have been identified, and in hexane in addition to MX and MX_2, there is evidence for the species MHX_2. Detailed studies and correlations are reported for the circular dichroism (CD), uv absorption, and fluorescence spectra of X-537A and X^- in solvents of different polarity and basicity, and of the various complexes of X-537A in methanol and hexane. The CD spectra are correlated in terms of a chemical model of three conformational tautomers of X-537A whose relative amounts depend on solvation and complexation. For K^+ and Ni^{2+} in methanol the changes in enthalpy and entropy for the complex formation have also been determined. The free energy of complexation is dominated by a positive entropy change. The role of solvation in stabilizing all these complexes is elucidated by analysis of the thermodynamics which is compared with similar treatment of the literature data for some other antibiotics.

The carboxylic ionophores, nigericin, dianemycin, monensin, X-537A (Figure 1), and X-206, comprise a subclass among the ion carrier antibiotics. They are chain-like molecules carrying polar groups (*e.g.*, hydroxyl, ether oxygen, carbonyl), one of which is a terminal carboxyl group. They can form cyclic structures which are stabilized by internal hydrogen bonding to the carboxyl group, especially when it is ionized. Also they are rather similar in respect to physiological activity in mitochondria, chloroplasts, chromatophores, bacteria, and other biological systems; their ionophoric capability makes them useful as probes of ion transport processes in these systems (Harris *et al.*, 1967; Cockrell *et al.*, 1967; Estrada *et al.*, 1967; Jackson *et al.*, 1968; Shavit *et al.*, 1970; Harold, 1972; Pressman, 1972).

Relatively distinct from the other carboxylic ionophores is X-537A (Berger *et al.*, 1951). It binds alkali metal ions, alkaline earth metal ions (Pressman, 1972; Degani *et al.*, 1973), rare earth metal ions (Pressman, 1973; Fernandez *et al.*, 1973), and transition metal ions. It also binds primary and secondary ammonium ions (Pressman, 1972). Thus it is useful for studying the role of Ca^{2+} in physiological systems such as sarcoplasmic reticulum (Scarpa and Inesi, 1972; Entman *et al.*, 1972; Caswell and Pressman, 1972), nerve terminals (Kita and Van der Kloot, 1974), rabbit heart (Pressman, 1972), and even living dogs (De Guzman and Pressman, 1974).

The actual mechanism of transport by the ion carriers in a biological process can be discussed in terms of several steps: (1) formation of a carrier–metal complex either in solution or at the interface of the membrane and the solution; (2) transport of the complex through the membrane; (3) dissociation of the metal from the carrier, either in solution or at the other membrane–solution interface; (4) transport of the carrier back through the membrane.

The characteristic ion selectivity of each antibiotic is similar in its biological activity and in solution, indicating that the overall efficiency of the transport is determined by important contributions from step 1 or 3 or both. Moreover, in some ways steps 1 and 3 are similar to the corresponding formation and dissociation processes in homogeneous solutions. These observations motivated the work reported here in which we determine the stoichiometries and stabilities of complexes of X-537A with various metal ions in methanol and in hexane. The solvents were selected to bracket the solvent properties of the interior of the phospholipid bilayer, methanol being more polar than the bilayer interior, while ionic solutes are less stable in hexane than in the interior of the phospholipid bilayer. Part of this work provides the basis for the studies of rates of complex formation with X-537A in methanol which are described in a later paper.

In describing the chemistry of X-537A it is quite necessary to specify its state of acid dissociation, hence we adopt the following notation. XH represents the acid form of X-537A, X^- is the anion, and the acid dissociation reaction is written

$$XH \longrightarrow H^+ + X^- \quad (1)$$

Similarly KX is the potassium complex and the reaction in which it is formed is written

$$XH + K^+ \rightleftharpoons H^+ + KX \quad (2)$$

or

$$X^- + K^+ \rightleftharpoons KX \quad (3)$$

according to the actual net process.

Experimental Section

Materials

Solvents. Spectro-analyzed methanol containing less than 0.04% water and certified *n*-hexane 99 mol % pure were obtained from Fisher Scientific Co. Other solvents were purified by standard methods (Perrin *et al.*, 1966).

† From the Department of Chemistry, State University of New York, Stony Brook, New York 11794. *Received June 6, 1974.* This work was supported by grants from the National Science Foundation (GP 31213), the National Institutes of Health (1 RO1 HL16474-01), and the U. S. Public Health Service Biomedical Sciences Support Grant (5 SO5 RR07067-07).

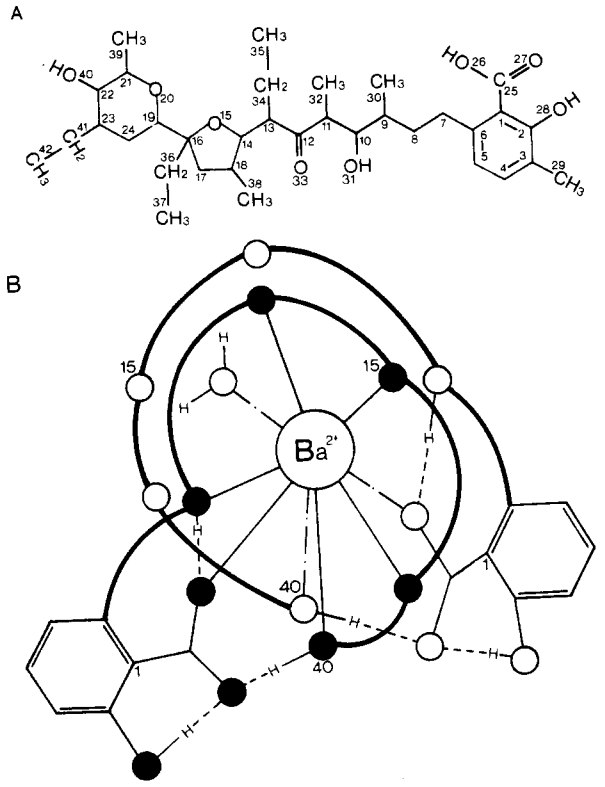

FIGURE 1: (A) X-537A. (B) Schematic drawing of BaX_2 based on the structure in the crystal (Johnson *et al.*, 1970).

Chemicals. Lithium chloride, ultra pure, lithium hydroxide, and anhydrous manganese chloride and nickel chloride were obtained from Alfa Inorganics, and Ultra pure rubidium chloride and cesium chloride were obtained from E. Merck. Other salts used were A.C.S. grade and were not further purified.

Methods

Uv absorption was measured with a Cary 15 spectrophotometer. Circular dichroism (CD) was measured with a Cary 60 spectrophotometer with a 6001 CD attachment. In each experiment the instrument was calibrated for zero ellipticity of the solvent and all solutes except X-537A. Two to three runs were performed for each measurement, the greatest difference in ellipticities at the extrema was 2×10^{-3} deg and the greatest difference in position of wavelength of extrema was 2 nm. Cylindrical quartz cells from Opticell were used, with light path ranging from 2 mm to 5 cm. Fluorescence was measured with an Aminco-Bowman spectrofluorimeter. The procedures for blanks were the same as for the CD measurements. The thermostated fluorescence cell chamber was controlled to ±1.5° as measured in the cell. For pH measurements a Radiometer pH meter with a combination electrode from Markeson Science Inc. was used. For studies in methanol, it was calibrated (±0.1 pH unit) with solutions of succinate and oxalate buffers, following the techniques of De Lingy *et al.* (1960). The pH values for the oxalate and succinate buffers at several methanol–water mixtures are given in Figure 2. Solutions of X-537A in methanol (without added base) were found to be stable, while in water and hexane there is a slow chemical change which gives rise to an absorption peak near 280 nm. Therefore, all solutions containing X-537A were freshly prepared prior to each experiment and checked for purity by absorption spectra.

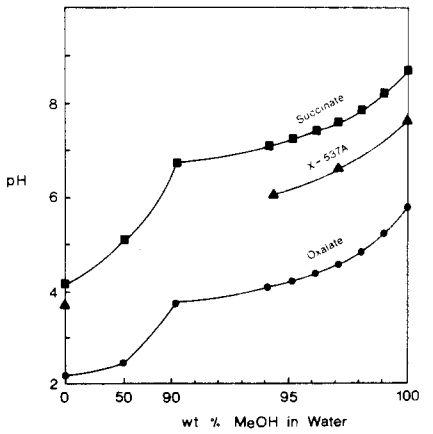

FIGURE 2: pK_a of XH as a function of methanol concentration at 25°. (▲) pH readings for solutions containing equimolar concentrations of XH and X^- (see Stoichiometry and Thermodynamics Section). The pH was adjusted with LiOH and $HClO_4$. The pH was calibrated at each methanol concentration using (■) equimolar succinic acid and lithium hydrogen succinate (10^{-2} M). To test the method the pH of (●) equimolar oxalic acid and the ammonium hydrogen oxalate (10^{-2} M) was also measured. Agreement with the literature values is exact in the scale of the graph.

Partition equilibrium was measured by mixing a hexane solution of X-537A with the same volume of buffered aqueous solution of known pH and salt concentration. After stirring the two-phase mixture for 75 sec, the phases were separated, and samples were taken for spectroscopic measurements. Preliminary studies had established that partition equilibrium is attained in 60 sec of stirring in a similar procedure. The buffer was either Tris (less than 5×10^{-3} M) or NaH_2PO_4–Na_2HPO_4 at a cation concentration of less than 10^{-3} M in order to avoid significant formation of NaX.

Results

Spectral Observations. The absorption spectra, circular dichroism, and fluorescence of X-537A in the ultraviolet-visible range (220–450 nm) are all useful in characterizing its chemical state, although in complementary ways. The spectral data and our limited interpretations of them are collected together in this section, except that further interpretation of the CD spectra is given in a later section.

ABSORPTION SPECTRA. The uv absorption spectra of X-537A and its complexes are dominated by two bands (Figure 3). The one near 310 nm is attributed to ^1A–^1L_b transition (Platt's notation; Platt, 1949) while the one near 245 nm is attributed to the ^1A–^1L_a transition of the salicylic group. Another absorption due to the $^1A_2$–$^1A_1$ ($n \rightarrow \pi^*$) transition of the carbonyl group near 285 nm is expected but is too weak to be observed in the presence of the salicylic chromophore bands.

The strength of the ^1L_b transition is found to be weakly dependent on the solvent. For example, the extinction coefficients of XH at 317 nm are 4100 in methanol and 4470 in *n*-hexane. The peak absorption coefficients and the wavelength at which those are located are found to be the same for the metal complexes as for X^- in a given solvent. Thus the uv absorption strength and frequencies were found to be rather insensitive to complex formation and to changes of solvent. The blue shift, from 317 to 305 nm and from 247 to ~240 nm, occurring upon ionization of the antibiotic, is analogous to shifts reported previously for salicylic acid and salicylate anion, and their derivatives (Doub and Vanden-

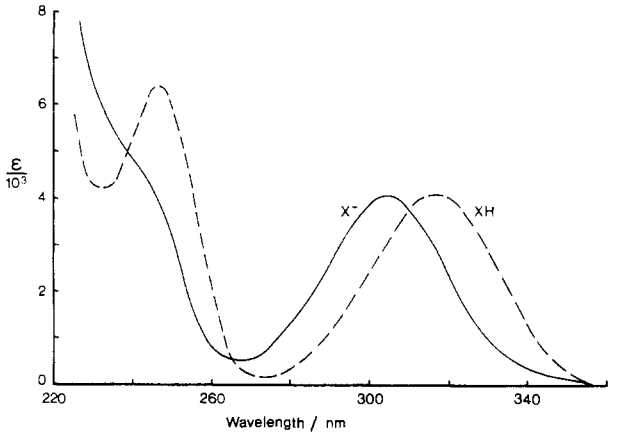

FIGURE 3: Absorption spectra in methanol solutions at 25° and 7.8 × 10^{-5} M X-537A. The X^- spectrum is for a solution at pH.10 (controlled by 10^{-4} M LiOH) while the XH spectra is for a solution at pH 4 (controlled by 10^{-3} M $HClO_4$).

belt, 1947, 1949, 1955). The effect on frequency shift of changing substituents on the benzene ring has been interpreted (Stevenson, 1965) in terms of inductive and conjugative effects of the substituents to perturb the states of benzene. For salicylic acid → salicylate the calculated shift is 6.7 nm for the ^1L_b transition in agreement with the observed shift of 6.5 nm. The dominant term in this calculation is the difference between the ortho correction for the hydrogen bonded pair COO^-–OH and COOH–OH. For COO^-–OH the strong hydrogen bond induces a larger ortho correction than for COOH–OH in which the hydrogen bond is weaker. Therefore, in salicylic acid and its derivatives this shift is mainly determined by the strength of the carboxyl–hydroxyl hydrogen bond. This conclusion indicates that the strength of the internal hydrogen bond ^{28}OH–^{27}O in X-537A does not depend much upon the solvent, since the spectral shift upon ionization is solvent independent. The ^1L_b and ^1L_a transitions of 3,6-dimethylsalicylic acid in methanol are at 315 nm with ε 4150, and at 246 nm with ε 7980; when KOH is added to the solution the ^1L_b peak is shifted to 305 nm with ε 3990 and the ^1L_a is shifted to a shoulder at 240.5 nm (Foye, 1968). These uv absorption characteristics are very similar to those found here for X-537A in similar solutions (Figure 3). This similarity confirms that the uv absorption method is not sensitive to conformational changes of X-537A.

CIRCULAR DICHROISM. In the CD spectra of X-537A and its metal complexes, there are two bands with extrema

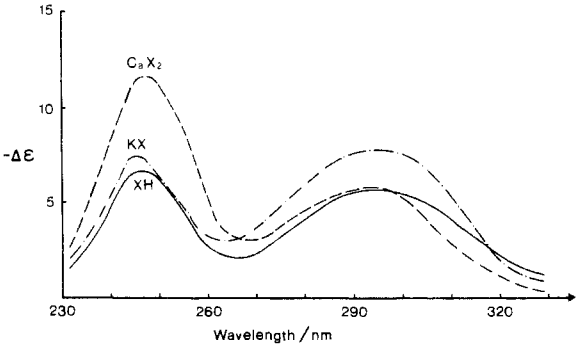

FIGURE 4: Circular dichroism in *n*-hexane solutions at 25° at 1.6 × 10^{-4} M stoichiometric concentration of X-537A. The KX and CaX_2 solutions were prepared by partition as described in the Experimental Section.

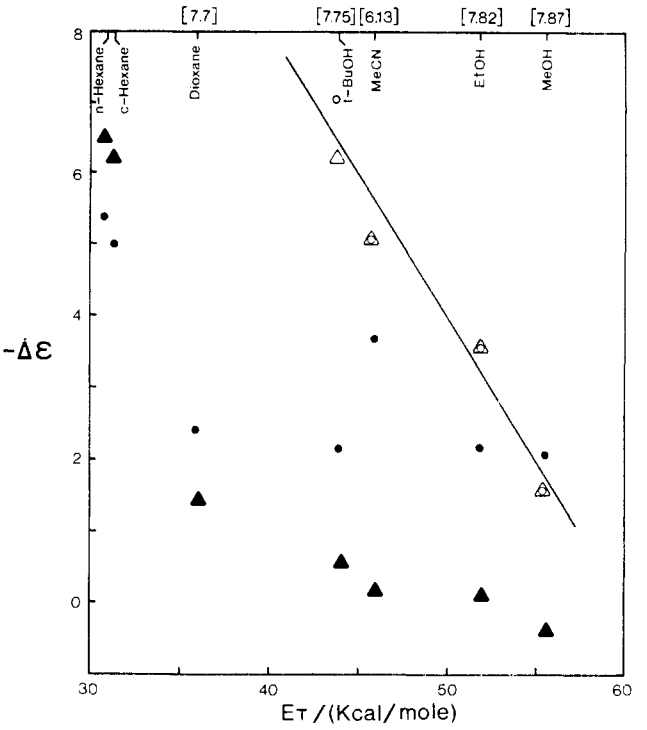

FIGURE 5: Solvation effects upon CD spectra of XH and X^-. (○,●) $-\Delta\epsilon$ at the extremum near 295, (△,▲) $-\Delta\epsilon$ at the extremum near 245 nm. Open figures for X^-, filled figures for XH. Solvent E_T data are from Reichardt and Dimroth (1968). The numbers in square brackets are solvent basicities (Krishnan and Friedman, 1971) given in terms of ΔH of the desolvation of normal alcohols extrapolated to zero length of the alkyl chain. The basicity of *t*-BuOH was assumed to be as that for *n*-BuOH, and the basicity of dioxane was determined from its correlated Donor Number (Gutmann, 1968).

at 290 ± 5 and 245 ± 5 nm (Figure 4). The molar CD absorption coefficients $\Delta\epsilon$ were calculated from the measured ellipticities according to the standard definition (Velluz *et al.*, 1963). Here $\Delta\epsilon$ is the effect per mole of X-537A, whether XH, KX, or ½ CaX_2, rather than per mole of compound (*i.e.*, KX, CaX_2). From 2 × 10^{-5} to 10^{-3} M, Beer's law is obeyed within the experimental error (10%). The sharp band at 245 nm which has negative $\Delta\epsilon$ in all systems studied except for XH and KHX^+ in methanol is associated with the ^1L_a transition of the salicylic group. The 290-nm band which has negative $\Delta\epsilon$ except for LiX in methanol may be associated with both the ^1L_b salicylic transition and the n → π* carbonyl transition. Its position and the fact that its changes are not correlated with those of the 245-nm band suggest that it is dominated by the n → π* carbonyl transition.

There are remarkably large solvent effects upon the amplitude of the CD of X^- and XH as shown in Figure 5. The corresponding shifts in wavelength extrema are relatively unimportant. The CD coefficients of the metal ion complexes in methanol and *n*-hexane are given in Figures 6 and 7, respectively.

Optical activity in X-537A and its complexes is induced by asymmetry of the molecular environment of each chromophore; CD effects therefore are sensitive to the changes in conformation of X-537A which are induced by changes in its solvation or complexation. Thus we may interpret the data in Figure 5 in terms of changes in conformation due to changes in solvation. To do so, however, we must distinguish between confusingly similar solvent characteristics, namely polarity and basicity. We take solvent polarity to be the medium's response to the field of an electric dipole

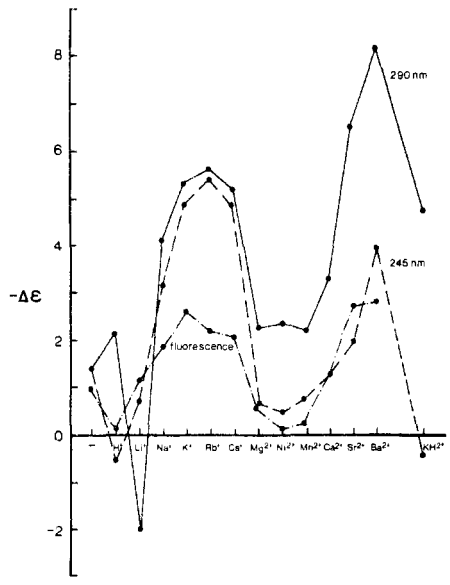

FIGURE 6: CD coefficients ($-\Delta\epsilon$) near 290 and 245 nm and relative fluorescence for X^-, MX complexes, MX^+ complexes, and the KHX^+ complex in methanol at 25°. The scale for the relative fluorescence is the same as for $-\Delta\epsilon$.

within a solute molecule; it is measured by Kosower Z values (Kosower, 1958) or E_T values (Reichardt and Dimroth, 1968). On the other hand, solvent basicity is defined in terms of the medium's ability to solvate an acidic atom or group, typically the hydroxyl group of an alcohol (Arnett, 1963; Krishnan and Friedman, 1971). While solvent basicity doubtless should be measured in terms of the free energy of solvation of the acidic group chosen as a probe, it is assumed that for a given acidic group and a series of rather similar solvents, the enthalpy of solvation of the acidic group is also a useful measure.

It may be recalled that within the BaX_2 complex in the crystal there are three hydrogen bonds (Figure 1B), ^{26}O–$H^{31}O$, ^{27}O–$H^{40}O$, ^{27}O–$H^{28}O$. The more basic the solvent the more it competes with the carboxyl oxygens ^{26}O and ^{27}O for the hydrogen bonds with the two hydroxyl groups ^{31}O, ^{40}O. (The ^{27}O–$H^{28}O$ hydrogen bond is strong and seems to be independent of the solvent as discussed previously.) That the carboxylate in X^- is a stronger hydrogen bond acceptor than the carboxyl of XH may explain why the conformation of X^- depends only on solvent polarities (E_T) while the conformation of XH depends on solvent basicity as well (Figure 5). Thus for X^- these data indicate that the solvent's ability to compete with internal hydrogen bonding is small and thus its basicity is unimportant in determining ionophore conformation. On the other hand, for XH the competition between internal hydrogen bonding and hydrogen bonding to the solvent is important, and solvent basicity has a marked effect on ionophore conformation.

Conformational changes are further discussed later where data for the metal-ion complexes of X-537A are included.

FLUORESCENCE. The excitation and emission spectra of XH and X^- in methanol are given in Figure 8 while data for the relative fluorescence intensity for all the principal complexes at the same concentration are summarized in Figure 6. The relative fluorescence is defined by

$$\text{relative fluorescence} = \frac{I_x^f(\lambda_x^f)/I_x^e(\lambda_x^e)}{I_{ref}^f(\lambda_{ref}^f)/I_{ref}^e(\lambda_{ref}^e)}$$

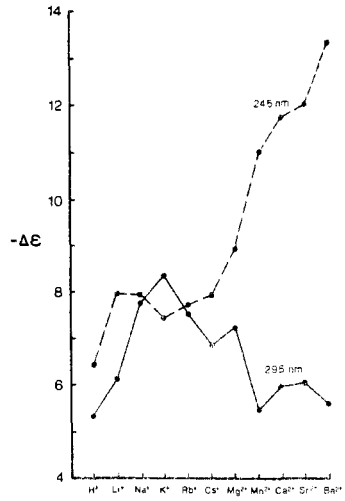

FIGURE 7: CD coefficients for XH, MX complexes, and MX_2 complexes in n-hexane at 25°. The ion complexes were prepared by partition as described in the Experimental Section.

where x refers to the particular species and ref refers to the reference species (X^- in methanol), I^e is the intensity of the exciting light absorbed in the sample and I^f is the intensity of the fluorescent light emitted by the sample, λ^e and λ^f are the excitation wavelength and fluorescence emission wavelength, respectively. In Figure 6 $\lambda_x = \lambda_{ref}$ for both the excitation and emission wavelengths. The measured fluorescence intensities of X^- and XH in methanol were found to obey Beer's law in the concentration range 10^{-6}–10^{-5} M (for a 1-cm light path). At higher concentrations there were large apparent deviations, possibly due to instrumental effects. For X^- and all the metal complexes the wavelengths for maximum excitation and maximum emission are 310 ± 5 and 420 ± 5 nm, respectively. For XH there is a shift of the emission peak to 380 ± 5 nm and a decrease in fluorescence intensity.

The fluorescence properties of X-537A, like the CD, are found to be very sensitive to the complexing metals. The changes induced upon ionization are also remarkably large and induce both a shift of the emission spectrum and a change in the intensity. Generally the relative fluorescence

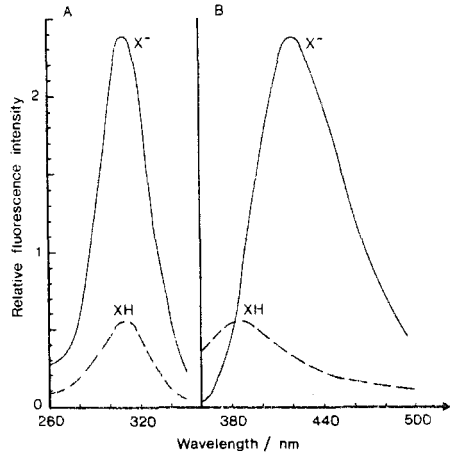

FIGURE 8: Excitation (A) and emission spectra (B) of fluorescence of X^- and XH in methanol at 25° (uncorrected). 2.7×10^{-5} M X-537A, cell path length 2.5 nm. X^- solutions controlled with 3×10^{-5} M LiOH, XH solutions controlled with 2×10^{-2} M $HClO_4$. The relative emission intensity for XH has been multiplied tenfold. Emission wavelengths for the excitation spectra: 420 nm and 380 nm for X^- and XH, respectively. Excitation wavelength for the emission spectra: 310 nm for both X^- and XH.

TABLE I: Formation Constants in Methanol at 25°.[a,b]

	Ion											
	H^+	Li^+	Na^+	K^+	Rb^+	Cs^+	Mg^{2+}	Ca^{2+}	Sr^{2+}	Ba^{2+}	Mn^{2+}	Ni^{2+}
pK	−7.6	−1.68	−2.57	−3.58	−3.56	−3.43	−3.83	−4.57	−5.47	−6.46	−4.40	−3.95
Ionic radius (Å)		0.60	0.95	1.33	1.48	1.69	0.65	0.99	1.13	1.35	0.80	0.73

[a] The constants for the sequence from Li^+ to Ba^{2+} were reported earlier (Degani *et al.*, 1973). [b] Here and elsewhere in this paper the reaction thermodynamics are expressed with respect to hypothetical 1 M standard states in the specified solvents. The standard states are often specified implicitly by incorporating units in the value of the equilibrium constant. For example, one might write for H^+ that $K = 10^{7.6}$ M^{-1}.

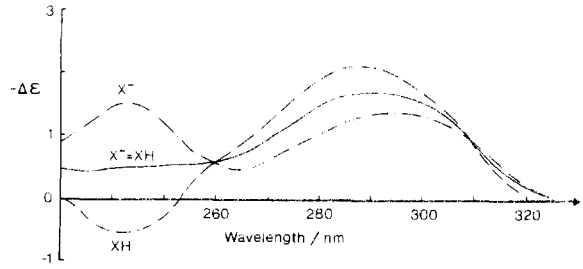

FIGURE 9: CD spectra in methanol solutions at 25° and 1.9×10^{-4} M X-537A. "XH" is a solution at pH 2.3 controlled with 10^{-2} M $HClO_4$. "X^-" is a solution at pH 9.7 controlled with 2×10^{-4} M LiOH. "X^- = XH" is a solution at pH 7.6 controlled with 2×10^{-6} M $HClO_4$ and 10^{-6} M LiOH.

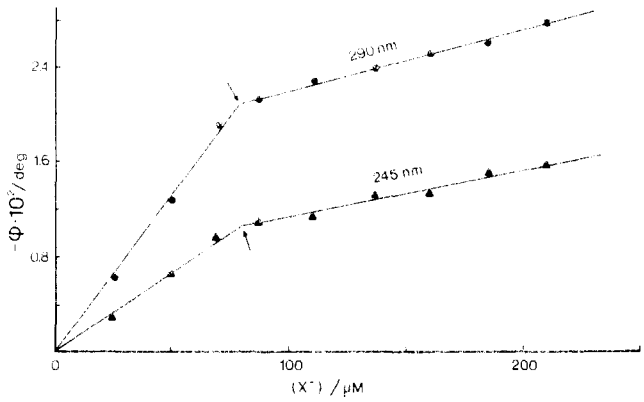

FIGURE 10: Ellipticity of the Ba^{2+} complex in methanol at 25° as a function of X^- concentration. $BaCl_2$ concentration constant at 80 μM. The arrows indicate the equivalence points.

intensities are correlated with the 245-nm CD coefficients (Figure 6). A more detailed study of fluorescence quantum yields and corrected spectra is needed for a quantitative discussion.

Stoichiometry and Thermodynamics. COMPLEXES IN METHANOL. By studying the spectra as a function of solution composition and analyzing in terms of the law of mass action it was established that for the metal ion species in Table I the dominant reaction is

$$M^{n+} + X^- \rightleftharpoons MX^{(n-1)+} \quad (4)$$

with the equilibrium constants given in Table I. Some general aspects, typical composition dependence studies, and special problems are discussed next.

The determination of the equilibrium for the reaction in methanol (eq 5) was already discussed in the Experimental

$$XH \rightleftharpoons X^- + H^+ \quad (5)$$

Section, except for the method of determining the $(X^-)/(XH)$ ratio in the solution. This was done by means of the CD spectra, as illustrated in Figure 9, except for pure water as the solvent. In that case, owing to the low solubility of XH, the CD method was relatively inaccurate and the $(X^-)/(XH)$ ratio was determined by the absorption spectrum near 310 nm.

The equilibrium constants for complex formation (eq 4) in methanol which are given in Table I were determined by studies of the composition dependence of the CD spectra. The 1:1 stoichiometry was established by fitting to the mass action law. For verification for Ca^{2+} and Ba^{2+} the stoichiometry was determined by the molar ratio method (Yoe and Jones, 1944) as illustrated in Figure 10.

To ensure that incomplete ionization of XH did not interfere in these studies, base was added so the final pH was larger by more than 2 pH units than the pK_a of XH. The base was either lithium hydroxide at a concentration low enough so LiX formation was negligible, or tributylamine (TBA). In order to test the possibility of complexation of $TBAH^+$ by X^-, additional $TBAH^+$ was added to solutions containing X^-. No changes in CD were observed (Table II). To see whether there might be significant amounts of a $TBAH^+X^-$ complex with the same spectral properties as X^-, the competition of K^+ with $TBAH^+$ was studied (Table II). Apparently the amount of $TBAH^+X^-$ complex formed, if any, is not great enough to interfere with the determination of the constants in Table I.

Traces of water (up to 5%) in methanol did not affect the equilibrium constant of the K^+ complex. On the other hand, water does affect the CD spectrum of the free antibiotic in pure methanol; the changes indicate that H_2O is merely acting as a base.

The results in Table I were largely confirmed by additional CD studies at lower pH, including some in which the only solutes were XH and the metal halide. However, these studies at lower pH also led to the discovery of a new type of complex with the formula MHX^+, when M is an alkali metal ion. The equilibrium constant of the reaction in methanol (eq 6) is $(1.8 \pm 0.3) \times 10^2$ at 25° as determined by

$$XH + K^+ \rightleftharpoons KHX^+ \quad (6)$$

studying the composition dependence of the CD spectra. The other MHX^+ formation constants have not been determined.

For K^+ and Ni^{2+} complexes in methanol the temperature dependence of the formation reaction was studied with the results given in Table III.

COMPLEXES IN HEXANE. The equilibrium constants for the two-phase reaction (eq 7) where $n = 1$ for alkali metal

$$nXH(\text{hexane}) + M^{n+}(\text{aq}) \rightleftharpoons MX_n(\text{hexane}) + nH^+(\text{aq}) \quad (7)$$

TABLE II: Ellipticity in Solutions of X^-, KX, and $TBAH^+$ in Methanol at 25°.[a]

KCl (M)	$TBAH^+$ (M)	2500ψ (deg) 295 nm	245 nm
		1.1 ± 0.2	1.1 ± 0.2
	1.0×10^{-3}	1.0	1.1
2.6×10^{-3}		5.5	4.3
2.6×10^{-3}	1.0×10^{-3}	5.1	4.4
7.4×10^{-4}		4.0	2.8
7.4×10^{-4}	2.3×10^{-3}	3.9	2.4

[a] $(X^-) = 9.2 \times 10^{-5}$ M; (TBA) = 4×10^{-8} M.

TABLE III: Temperature Dependence of Formation of $MX^{(n-1)+}$ in Methanol (eq 4).

	Temp (°C) 2	25	46
K^+, pK_4	−3.77	−3.58	−3.33
Ni^{2+}, pK_4	−4.10	−3.96	−3.85

Thermodynamics at 25°

	$\Delta G°$ (kcal/mol)	$\Delta H°$ (kcal/mol)	$\Delta S°$ (cal/(mol deg))
K^+	−3.58 ± 0.02	4.1 ± 1.1	26 ± 4
Ni^{2+}	−5.40 ± 0.02	2.3 ± 0.1	26 ± 1

ions and $n = 2$ for the alkaline earth metal ions and Mn^{2+} are given in Table IV. The proton concentration in the water phase was controlled by buffers. The stoichiometries were found by the same methods as previously described for methanol.

At relatively low ($<10^{-2}$ M) concentration of Cs^+ in the water phase, an apparent enhancement of $-\Delta\epsilon$ at 245 nm of CsX was observed. This could be explained by formation of a complex with the formula $CsHX_2$. It is the neutral equivalent of the MHX^+ complexes found in methanol.

CD Spectra and Molecular Conformation. As already pointed out it is expected that the CD spectra of X-537A and its derivatives are sensitive to conformation. This expectation has led to an effort to develop a "chemical model" for the interpretation of the CD spectra. Thus we now assume that there is some number of conformational tautomers of X^-, each with its characteristic CD spectrum. Solvation and complexation, whether by metal ions or by H^+ (to form XH), are assumed to stabilize the conformers to different degrees but not to affect the spectra of the individual conformers. Thus the model attributes the observed changes in spectra to changes in the relative proportion of the conformers. It will be useful if it enables us to systemize the data; also it may provide a basis for interpretation and prediction.

Our hypothesis is that there are three dominant conformers of X-537A: (I) Open-chain conformation with one internal hydrogen bond (^{27}O–$H^{28}O$). The CD coefficients of the two bands are near zero. (II) "Partial" ring conformation having two hydrogen bonds (^{27}O–$H^{28}O$, ^{26}O–$H^{31}O$). It has a negative $\Delta\epsilon$ in the 290-nm CD band and a small positive $\Delta\epsilon$ in the 245-nm CD band. (III) A ring conformation held by head to tail hydrogen bond (^{27}O–$H^{40}O$) and the two other possible hydrogen bonds. In this conformation the exterior "surface" of the molecule is all hydrophobic. It has large values of $-\Delta\epsilon$ for both CD bands.

Based on these postulates the conformer composition of the various complexes of X-537A in various solvents can be assigned as shown in Table V.

For X^- the two CD bands are nearly the same in methanol, ethanol, acetonitrile, and *tert*-butyl alcohol. The two dominant conformers seem to be I and III, shifting in favor of III with decreasing solvent polarity. Binding of X^- by H^+ reduces $-\Delta\epsilon$ in the 240-nm CD band to zero and even to a small positive value in methanol. This change indicates that the dominant conformers in XH are I and II. The relative amount of each conformer depends mostly on the solvent basicity, hence for all the more basic solvents (methanol, ethanol, *tert*-butyl alcohol, and 1,4-dioxane) the CD spectrum of XH is nearly the same. The small changes in the 245-nm band which are observed are attributed to variations in the small proportion of conformer III due to variations in solvent polarity. For acetonitrile, a relatively polar solvent but a poor hydrogen bond acceptor, the ratio of II to I is larger as shown by a larger $-\Delta\epsilon$ of the 290-nm CD band. This is attributed to a greater extent of internal hydrogen bond formation between ^{31}OH and the carboxyl group in this solvent. In the nonpolar hydrocarbon solvents, *n*-hexane and cyclohexane, the relatively large $-\Delta\epsilon$ of both CD bands indicates that where there is no competition with the solvent to form hydrogen bonds the dominant conformation is III.

The CD spectra of the MX complexes are almost independent of the solvent (except for the Li^+ complex), thus indicating that the conformation is controlled by the coordination to a metal ion, which would favor the ring structure III. The exceptional positive $\Delta\epsilon$ in the 290-nm CD band of LiX in methanol indicates that a special structure is formed for this complex, probably due to the small size of the ion.

In the CD spectra of the special group of alkali metal complexes MHX^+, only the 290-nm band is enhanced by complexation while the CD 245-nm band remains the same as for XH. This suggests that for these complexes the metal ion is coordinated to the same oxygens as for the MX complexes except that the salicylic group remains free and has

TABLE IV: Complex Formation in *n*-Hexane at 25°[a] (eq 7).

	Ion Li^+	Na^+	K^+	Rb^+	Cs^+	Mg^{2+}	Ca^{2+}	Sr^{2+}	Ba^{2+}	Mn^{2+}
pK	6.2	5.7	5.6	5.8	6.0	>8.4	7.5	6.8	3.7	7.8

[a] 1 M standard states in each phase. Error limit ±0.1 pK unit.

TABLE V: Dominant Conformers of X-537A Based on CD Data.

Species	XH	XH	XH	X^-	X^-
Solvent	Methanol	Acetonitrile	Hexane	Methanol	*t*-Butyl alcohol
Conformers[a]	I > II	II > I	III	I > III	III

Ion	Na^+	K^+	Rb^+	Cs^+	Mg^{2+} Ni^{2+} Mn^{2+} Ca^{2+}	Sr^{2+}	Ba^{2+}
Conformers in methanol	III > I	III	III	III	I > II ≃ III	II ≃ III > I	III > II

[a] For example, "I > II" means mainly conformer I, some conformer II, and no significant amount of conformer III.

the same environment as in conformer II.

The alkaline earth metal complexes have distinctively different CD characteristics in methanol and *n*-hexane, as expected for different stoichiometries which necessarily have different conformations. In methanol the 290-nm band is enhanced up to a factor of 4 for the Ba^{2+} complex, while the enhancement of the 245-nm band is smaller, only half of that value. As mentioned previously, for the alkali metal ions, the two bands were about equally enhanced. This difference suggests that for the MX^+ complexes in methanol appreciable amounts of II are present in addition to conformer III, thus causing a relative decrease in $-\Delta\epsilon$ at 245 nm. On the other hand, in *n*-hexane the 245-nm band of the MX_2 complexes is enhanced relative to that in XH up to a factor larger than 2 for the BaX_2 complex while only very small changes occur for the 290-nm band. The large enhancement of the 245-nm CD band is reminiscent of the large $|\Delta\epsilon|$ (10–20) reported for the 230-nm CD band of dibenzoates (Harada and Nakanishi, 1969).

For most of the dibenzoates a second CD band with a large amplitude but of opposite sign appears near 215 nm. This 215-nm CD band is not easily detectable in some dibenzoates nor in our case, either due to instrumental limitations, caused by a strong background ellipticity arising from the extremely strong benzene ring absorption near 200 nm, or deviations from the zero order approximation of the molecular exciton theory (Tinoco, 1962) used to interpret this phenomenon.

Role of Solvation in Stabilizing the Complexes. By comparing the thermodynamics of complexation in methanol (Table I) with the corresponding data in hexane (Table IV) we may learn about the role of solvation in the complexation process. We consider the alkali metal complexes first. For the others the interpretation is more difficult because the dominant complex is not the same in the two solvents. At the end of this section we analyze thermodynamic data for similar reactions of some other antibiotics in order to test the validity of our method.

The first step in the comparison is the use of ancillary data to obtain data for the analogous reactions in the two solvents. Data for the reaction in methanol (MeOH) (eq 8)

$$M^+(MeOH) + X^-(MeOH) \longrightarrow MX(MeOH) \quad (8)$$

are given in Table I while data for the reaction in hexane (hex) (eq 9) are given in Table IV; the two reactions are not

$$M^+(aq) + XH(hex) \longrightarrow H^+(aq) + MX(hex) \quad (9)$$

directly comparable. Since there are no thermodynamic data for ions in solution in hexane, we have no choice but to combine data for eq 8 with other data to obtain results for the reaction which is analogous to eq 9.

$$M^+(aq) + XH(MeOH) \longrightarrow H^+(aq) + MX(MeOH) \quad (10)$$

We need data for the reaction

$$XH(MeOH) \longrightarrow H^+(MeOH) + X^-(MeOH) \quad (11)$$

for which we found $pK \simeq 7.6$ as shown in Figure 2. We also need data for the reaction

$$M^+(aq) + H^+(MeOH) \longrightarrow M^+(MeOH) + H^+(aq) \quad (12)$$

for which the standard free energy change is just the standard free energy of transfer of M^+ from water to methanol, for which data are available (Kolthoff and Chantooni, 1972, *cf.* Table VI).

In order to avoid the use of unnecessary notation we notice that

$$pK_j = \frac{\Delta G^\circ_j \text{ in units of } RT}{2.303} \quad (13)$$

where K_j and ΔG°_j are respectively the equilibrium constant and the standard free energy change for the process in eq *j* with "hypothetical 1 molar" standard states, so p*K* values and ΔG° values are the same (at fixed temperature, here 25°) except for constant factors, and they can be discussed in the same way.

The use of the data reported here for eq 8 and 12 together with literature values for eq 10 leads to the results given in Table VI. The difference $pK_{10} - pK_9$ gives p*K* for eq 14

$$XH(MeOH) + MX(hex) \longrightarrow MX(MeOH) + XH(hex) \quad (14)$$

which also is given in Table VI. For eq 15 we estimate pK_{15}

$$XH(MeOH) \longrightarrow XH(hex) \quad (15)$$

$= -0.7 \pm 1$ on the basis that XH is about 1000 times more soluble in methanol than in water, whereas in the partition equilibrium between hexane and acidified (pH 5) water XH is about 5000-fold more concentrated in the hexane than in the water. While the uncertainty in pK_{15} is rather large it does not affect the trend in p*K* for the process (eq 16) given in Table VI.

$$MX(hex) \longrightarrow MX(MeOH) \quad (16)$$

In the very simple case in which the M^+ in MX is completely covered up by the X^- so that the solvent does not

TABLE VI: Free Energy Data for Alkali Metal Ions at 25°.

M^+	Li^+	Na^+	K^+	Rb^+	Cs^+
pK_{12}[a,b]	−0.4[c]	−0.4	−0.1	−0.1	−0.2
pK_{10}	5.5	4.6	3.9	3.9	4.0
pK_9	6.2	5.7	5.6	5.8	6.0
pK_{14}	−0.7	−1.1	−1.7	−1.9	−2.0
pK_{16}	0	−0.4	−1.0	−1.2	−1.3

[a] See eq 13 for explanation of pK_j notation. [b] Kolthoff and Chantooni, 1972. [c] Estimated to be the same as for Na^+; this is probably an upper limit for pK_{14} for Li^+.

"see" the M^+, we would expect pK_{16} to be nearly independent of M^+ and to be somewhat positive on the basis that the exterior of MX would be mainly hydrocarbon like and therefore better solvated by hexane than by methanol. To the degree that the X^- is not big enough and flexible enough to cover-up the M^+ and shield it from the solvent we would expect pK_{16} to be negative owing to M^+ being better solvated by methanol than by hexane.

These considerations show that the trend in pK_{16} values would be accounted for if the shielding of M^+ by X^- were rather complete in LiX and becoming less complete in the series from LiX to CsX. This is an expected steric effect.

This picture of the structure of MX differs in detail from that of Pressman who pictured it as M^+ sitting on a ring of ligating groups offered by X^- in a disc-like conformation (Pressman, 1972). If one allows a smaller M^+ to bury itself deeper among the ligating groups, then Pressman's model would be consistent with the data for pK_{16}, otherwise one would expect his model to show a trend in the opposite direction. Thus the thermodynamic data seem to support a conclusion about the structure of MX, namely, that the metal ion is only partially shielded from the solvent, and less so the larger the metal ion.

In Table VII, the M^{2+} ions for which we have data in both methanol and hexane are listed in order of increasing crystal radius together with pK values for the reaction

$$M^{2+}(MeOH) + X^-(MeOH) \longrightarrow MX^+(MeOH) \quad (17)$$

To proceed as before these data should be combined with the standard free energies of transfer of the metal ions from water to methanol. Unfortunately, there do not seem to be

$$M^{2+}(aq) + 2H^+(MeOH) \longrightarrow M^{2+}(MeOH) + 2H^+(aq) \quad (18)$$

any data for this process and it has been necessary to guess the values as shown in Table VII. Combined with data for eq 11 these estimates give pK for the reaction

$$M^{2+}(aq) + 2XH(MeOH) \longrightarrow MX^+(MeOH) + 2H^+(aq) + X^-(MeOH) \quad (19)$$

which is as near as we can come to the analog of

$$M^{2+}(aq) + 2XH(hex) \longrightarrow MX_2(hex) + 2H^+(aq) \quad (20)$$

for which we have the pK data in Table IV.

The algebraic combination (19) − (20) − 2(15) gives the net reaction

$$MX_2(hex) \longrightarrow MX^+(MeOH) + X^-(MeOH) \quad (21)$$

with results given in Table VII.

On the basis of experiments in which we attempted unsuccessfully to detect MX_2 in methanol solutions we estimate $pK < 3$ for the reaction

$$MX_2(MeOH) \longrightarrow MX^+(MeOH) + X^-(MeOH) \quad (22)$$

Considering the reaction

$$MX_2(hex) \longrightarrow MX_2(MeOH) \quad (23)$$

and assuming $C = 0$ (*cf.* Table VII) we find that $pK_{23} > 1.1$ for Ca^{2+} and $pK_{23} > 3.3$ for Ba^{2+}, so the undetectability of MX_2 in methanol is consistent with the expectation that $\Delta G°$ for eq 23 is positive (because of the hydrophobic nature of the MX_2 complex).

The pK_{21} data in Table VII indicate that in the case of Ba^{2+} compared to Sr^{2+} and Ca^{2+} the species MX_2 is markedly more stable relative to MX^+. This observation elucidates the great stability of BaX_2 compared to CaX_2 and SrX_2 shown in Table IV. There one might suspect that the extra stability really reflects poor hydration of Ba^{2+} relative to the others; however, such an interpretation would not explain the difference in pK_{21}. It must be concluded that the BaX_2 complex really is more stable than one would expect from trends in the series MgX_2, CaX_2, SrX_2. Perhaps the barium ion fits the hole between two X^- ions (Johnson *et al.*, 1970) much better than the smaller ions. It is remarkable that the extra stability of BaX_2 is not reflected by differences in the absorption spectra, CD spectra, or fluorescence.

TABLE VII: Analysis of the Stabilities of Some M^{2+} Complexes at 25°.

M^{2+}	Mg^{2+}	Mn^{2+}	Ca^{2+}	Sr^{2+}	Ba^{2+}
pK_{18}[a]	$C - 0.4$	$C - 0.4$	$C - 0.4$	$C - 0.1$	$C - 0.1$
pK_{17}	−3.8	−4.4	−4.6	−5.5	−6.5
pK_{19}	$C + 11$	$C + 10.4$	$C + 10.2$	$C + 9.6$	$C + 8.6$
pK_{20}	>8.4	7.8	7.5	6.8	3.7
pK_{21}	$<4.0 + C$	$4.0 + C$	$4.1 + C$	$4.2 + C$	$6.3 + C$

[a] The trend in this value is estimated by assuming that it is the same as the trend of pK_{12} (Table VI) for M^+ ions of similar radii. Thus C is a constant. It should be noted that the significance of the results in the last row of this table does not depend on this assumption unless the variation in pK_{18} is very much greater than we have assumed.

No experimental data are available for a similar analysis of the thermodynamics of complexing by the other carboxylic ionophores. However, for several cyclic noncarboxylic ionophores the experimental results found in the literature, although not complete, do enable us to analyze the role of solvation in stabilizing the complexes. For valinomycin (Val) there are data (Funck *et al.*, 1972) for the reaction

$$Val(MeOH) + M^+(MeOH) \longrightarrow ValM^+(MeOH) \quad (24)$$

and for the partition equilibrium (Eisenman *et al.*, 1973)

$$Val(CH_2Cl_2) + M^+(aq) + A^-(aq) \longrightarrow ValM^+A^-(CH_2Cl_2) \quad (25)$$

where A^- is picrate anion and $ValM^+A^-$ is an ion pair of $ValM^+$ with A^-.

In order to obtain results for the reaction

$$ValM^+A^-(CH_2Cl_2) + H^+(MeOH) \longrightarrow ValM^+(MeOH) + A^-(aq) + H^+(aq) \quad (26)$$

we notice that this is the algebraic combination of several other reactions as follows

$$(26) = (24) - (25) + (12) + (28) \quad (27)$$

where we write

$$Val(CH_2Cl_2) \longrightarrow Val(MeOH) \quad (28)$$

An estimate for pK_{28} follows from the solubility of Val in methanol, which is by a factor of 10^3–10^4 higher than in water, and the solubility of Val in CH_2Cl_2 which is 10^4 higher than in water, based on reported results for partition of Val between water and dioleoyllecithin in decane 0.3%, w/v (Stark and Benz, 1971). Hence $pK_{28} = 1.0 \pm 1.0$. The literature data for pK_{24} and pK_{25} and the results for pK_{26} are given in Table VIII.

The difference in pK_{26} for the complex of sodium and the three other alkali metal ions is remarkable. It indicates

TABLE VIII: Analysis of the Stabilities of Some M^+ Complexes of Valinomycin and Monactin at 25°.

	M^+	Na^+	K^+	Rb^+	Cs^+
Val	pK_{24}	−0.7	−4.5	−4.8	−3.9
	pK_{25}	0.8	−4.0	−4.4	−3.8
	pK_{26}	−0.9	+0.4	+0.5	+0.7
Mon	pK_{26}	−1.5	−1.6		

that a larger stabilization of the Na^+ complex is achieved in methanol due to the interaction with the solvent, while for the other ions the interaction with the solvent is smaller, and becomes more so with increasing ionic radius. That in $ValNa^+$ the Na^+ is not completely shielded by the Val is in full agreement with the results reported by Grell and Funck (1973) who interpret ^{13}C nmr and ir-absorption data to show that in the complexes of K^+, Rb^+, and Cs^+ there are six ester carbonyl groups coordinated to the metal ion, forming a rather rigid structure which is stabilized by the formation of six intramolecular hydrogen bonds between the amide groups. In contrast to these results the ligand conformation of the complex with Na^+ was reported to be considerably different; the number of coordinated ester groups and intramolecular hydrogen bonds is reduced leading to a less compact and less closed structure. Since not all of the ester oxygens were found to be coordinated to Na^+ and coordination of other groups could not be detected, it was furthermore assumed that the coordinated Na^+ ion might be partially solvated. This complementary agreement of the interpretation of thermodynamic properties and spectroscopy supports both interpretations.

The thermodynamic data (Wipf *et al.*, 1968; Eisenman *et al.*, 1969; Stark and Benz, 1971) for monactin (Mon) are less complete than for Val but can be analyzed in the same way. Using again eq 24 to 28 but replacing Val by Mon we obtain the results for monactin given in Table VIII. The results are just what would be expected if in both $MonNa^+$ and $MonK^+$ the metal ion were covered up by the monactin to the same extent.

Returning now to the thermodynamic data for X-537A in methanol, the data in Table III show that for the formation of K^+ and Ni^{2+} complexes, the main contribution to the favorable free energy change is from the entropy change rather than the enthalpy change. The entropy increase in the complexation must be attributed to the increase in entropy of the solvent when the metal ion is more shielded from the solvent by forming the complex MX or MX^+. It is of interest to examine these entropy changes more closely. The data can be combined to give $\Delta S = 0 \pm 5$ cal/(mol deg) for the following exchange reaction in methanol

$$Ni^{2+} + KX \longrightarrow K^+ + NiX^+ \quad (29)$$

This result may be compared with the reaction

$$Ni^{2+}(MeOH) + K^+(g) \longrightarrow Ni^{2+}(g) + K^+(MeOH) \quad (30)$$

for which we find $\Delta S = +54$ cal/(mol deg) by using the equation of Criss *et al.* (1968) to derive ionic entropies in methanol from the well-known ionic entropies in water (Friedman and Krishnan, 1973). In reaction 30 the ΔS reflects the difference in solution entropies of K^+ and Ni^{2+}. If the metal ion were completely desolvated in forming the respective complexes, KX and NiX^+, we would expect ΔS for reaction 29 to be comparable to that for reaction 30 because

TABLE IX: Enthalpy and Entropy for the Complexation of Ionophores with Alkali Metal Ions in Methanol at 25°.

Ionophore	Ion	$\Delta G°$ (kcal/mol)	$\Delta H°$ (kcal/mol)	$\Delta S°$ (cal/(mol deg))
Nigericin[a]	Na^+	−5.6	1.64	24
	K^+	−7.9	−0.98	23
Monensin[a]	Na^+	−8.5	−3.87	15
	K^+	−6.5	−3.73	9.5
Valinomycin[b]	K^+	−8.3	−8.9	−2.2
Nonactin[c]	K^+	−6.1	−10.97	−16.4
Dicyclo-30-crown 10[d]	Na^+	−2.9	−4.0	−3.7
	K^+	−6.2	−11.5	−17.8
	Rb^+	−6.3	−12.7	−21.4
	Cs^+	−5.8	−11.2	−18.1
Dicyclohexyl-18-crown-6 (isomer B)[e]	Na^+	−5.0	−5.6	−2.0
	K^+	−7.4	−10.5	−10.4

[a] Lutz *et al.*, 1971. [b] Moeschler *et al.*, 1971, in ethanol. [c] Frueh *et al.*, 1971. [d] Chock, 1972. [e] Christensen *et al.*, 1971.

it seems unlikely that more than a small fraction of the entropy effect due to the polarization of the solvent in the field of an ion can be compensated (in eq 29) by the polarization of X^- in the field of the ion. Therefore, the large difference in ΔS between eq 29 and 30 can only mean that the metal ions in KX and NiX^+ are still rather strongly solvated by methanol and this ionic solvation is relatively more important in NiX^+ than in KX, probably due to differences in the charge and conformation of the two complexes. Comparison of the $\Delta\epsilon$'s for these complexes in methanol (Figure 6) supports the conclusion derived from the thermodynamic data. On the basis of the chemical model for the CD effects (Table V) the spectral differences imply that K^+ in KX (dominant conformation III) is considerably better shielded by the ionophore than Ni^{2+} in NiX^+ (all three conformers present) from interacting with the methanol solvent.

The thermodynamic data for complexation of M^+ ions by several other natural or synthetic ionophores (Table IX) show that $\Delta S°$ is very much greater for the carboxylic ionophores (nigericin and monensin as well as X-537A) than for the others. It must be remarked that the difference in sign of $\Delta S°$ for the carboxylic ionophores compared to the others is an accident due to the choice of standard states. Thus for 1 μM standard states, rather than 1 M, all of the $\Delta S°$ values in Table IX would be 27.4 cal/(mol deg) more negative than the values given; they would all be negative.

To remove the dependence on standard states we may examine an exchange reaction such as the reaction in methanol (eq 31) where Non = nonactin and where we have (Tables III and IX) $\Delta S°_{31} = -42$ cal/(mol deg).

$$KX + Non \longrightarrow NonK^+ + X^- \quad (31)$$

There is a contribution to $\Delta S°_{31}$ due to the polarization of the solvent by the ions. By means of the Born equation this may be estimated, for each ion of radius r_i and charge e_i, as

$$\Delta S_B = -\frac{e^2}{2r_i D}\frac{\partial \ln D}{\partial T} \quad (32)$$

where D is the dielectric constant of the solvent. For $r_i \sim 7$ Å, as for $NonK^+$, and $\partial \ln D/\partial T = -6 \times 10^{-3}$ (Dannhauser and Bahe, 1964), we would calculate $\Delta S_B = -5$ cal/

(mol deg). Thus the "ionic" contribution to $\Delta S°_{31}$, as estimated by the Born charging equation, is only about −10 cal/(mol deg), leaving about −30 cal/(mol deg) to be accounted for in terms of specific solvation and conformational effects in the antibiotics.

Comparison with Earlier Studies of X-537A. The role of X-537A as an ionophore in model and biological systems was studied extensively by Pressman and coworkers (Pressman, 1969, 1972, 1973). The partition reaction, eq 7, but with 30% 1-butanol in toluene in place of hexane, was investigated (Pressman and Haynes, 1969; Pressman, 1972). The equilibrium constants given in relative units (relative to K^+ for the alkali metal ions and to Ca^{2+} for the alkaline earth metal ions) are generally in agreement with those for hexane given in Table IV. This indicates that addition of a basic cosolvent such as 1-butanol to toluene has only a small effect on the stability of MX or MX_2. Thus hexane as well as toluene–butanol mixtures can serve as a model of the membrane interior.

Fluorescence and preliminary CD measurements reported previously (Entman *et al.*, 1972; Caswell and Pressman, 1972; Degani *et al.*, 1973; Haynes and Pressman, 1974) are in agreement with the present data.

As the present work was completed a report of the spectra of X-537A and its complexes in ethanol and heptane appeared (Alpha and Brady, 1973) with results which apparently disagree with ours to a much greater extent than one could expect from the differences in solvents. Unfortunately, it is very difficult to make a quantitative comparison and to analyze the possible sources of the discrepancies due to some internal inconsistencies and lack of specification of the equilibrium concentrations of species in the solutions of which the spectra are determined.

Acknowledgments

We thank Dr. J. Berger of Hoffman-La Roche for supplying antibiotic X-537A, Professor E. M. Kosower for his advice and encouragement during the early stages of this work, Professor S. R. Simon for use of his laboratory, and we thank him with Professor S. R. McLaughlin and Dr. C. V. Krishnan for many helpful discussions.

References

Alpha, S. R., and Brady, A. H. (1973), *J. Amer. Chem. Soc. 95,* 7043.

Arnett, E. M. (1963), *Progr. Phys. Org. Chem. 1,* 223.

Berger, J., Rachlin, A. I., Scott, W. E., Sternbach, L. H., and Goldberg, M. W. (1951), *J. Amer. Chem. Soc. 73,* 5295.

Caswell, A. H., and Pressman, B. C. (1972), *Biochem. Biophys. Res. Commun. 49,* 292.

Chock, P. B. (1972), *Proc. Nat. Acad. Sci. U. S. 69,* 1939.

Christensen, J. J., Hill, J. O., and Izatt, R. M. (1971), *Science 173,* 1252.

Cockrell, R. S., Harris, E. J., and Pressman, B. C. (1967), *Nature (London) 215,* 1487.

Criss, C. M., Held, R. P., and Liksha, E. (1968), *J. Phys. Chem. 72,* 2970.

Dannhauser, W. and Bahe, L. W. (1964), *J. Chem. Phys. 40,* 3058.

Degani, H., Friedman, H. L., Navon, G., and Kosower, E. M. (1973), *J. Chem. Soc., Chem. Commun.,* 432.

De Guzman, N. T., and Pressman, B. C. (1974), *Circulation 46,* 1072.

De Lingy, C. L., Luykx, P. F. M., Rehbach, M., and Wieneke, A. A. (1960), *Recl. Trav. Chim. Pays-Bas 79,* 713.

De Lingy, C. L., and Wieneke, A. A. (1960), *Recl. Trav. Chim. Pays-Bas 79,* 268.

Doub, L., and Vandenbelt, J. M. (1947), *J. Amer. Chem. Soc. 69,* 2714.

Doub, L., and Vandenbelt, J. M. (1949), *J. Amer. Chem. Soc. 71,* 2414.

Doub, L., and Vandenbelt, J. M. (1955), *J. Amer. Chem. Soc. 77,* 4535.

Eisenman, G., Ciani, S. M., and Szabo, G. (1969), *J. Membrane Biol. 1,* 294.

Eisenman, G., Szabo, G., McLaughlin, S. G. A., and Ciani, S. M. (1973), *J. Bioenerg. 4,* 93.

Entman, M. L., Gillette, P. C., Wallick, E. T., Pressman, B. C., and Schwartz, A. (1972), *Biochem. Biophys. Res. Commun. 48,* 847.

Estrada, O. S., Graven, S. N., and Lardy, H. A. (1967), *J. Biol. Chem. 242,* 2925.

Fernandez, M. S., Celis, C. H., and Muntal, M. (1973), *Biochim. Biophys. Acta 323,* 600.

Foye, W. O. (1968), The Sadtler Standard Spectra, Ultraviolet, Vol. 55, No. 13310.

Friedman, H. L., and Krishnan, C. V. (1973), *in* Water, Vol. 3, Franks, F., Ed., New York, N.Y., Plenum Publishing Co., Chapter 1.

Frueh, P. U., Clerc, J. T., and Simon, W. (1971), *Helv. Chim. Acta 54,* 1445.

Funck, T., Eggers, F., and Gress, E. (1972), *Chimia 26,* 637.

Grell, E., and Funck, T. (1973), *Eur. J. Biochem. 34,* 415.

Gutmann, V. (1968), Coordination Chemistry in Non-Aqueous Solutions, New York, N.Y., Springer-Verlag, Chapter II.

Harada, N., and Nakanishi, K. (1969), *J. Amer. Chem. Soc. 91,* 3989.

Harold, F. M. (1972), *Bacteriol. Rev. 36,* 172.

Harris, E. J., Hofer, M. P., and Pressman, B. C. (1967), *Biochemistry 6,* 1348.

Haynes, D. H., and Pressman, B. C. (1974), *J. Membrane Biol. 16,* 195.

Henderson, P. J. F., McGivan, J. D., and Chappell, J. B. (1969), *Biochem. J. 111,* 521.

Jackson, J. B., Crofts, A. R., and Von Sredingk, L. V. (1968), *Eur. J. Biochem. 6,* 41.

Johnson, M. S., Herrin, J., Liu, J. S., and Paul, I. C. (1970), *J. Amer. Chem. Soc. 92,* 4423.

Kita, H., and Van der Kloot, W. (1974), *Nature (London)* (in press).

Kolthoff, I. M., and Chantooni, Jr., M. K. (1972), *J. Phys. Chem. 76,* 2024.

Kosower, E. M. (1958), *J. Amer. Chem. Soc. 80,* 3253.

Krishnan, C. V., and Friedman, H. L. (1971), *J. Phys. Chem. 75,* 3598.

Lutz, W. K., Fruh, P. V., and Simon, W. (1971), *Helv. Chim. Acta 54,* 1437.

Moeschler, H. J., Weder, H. G., and Schwyzer, R. (1971), *Helv. Chim. Acta 54,* 1437.

Perrin, D. D., Armarego, W. L. F., and Perrin, D. R. (1966), Purification of Laboratory Chemicals, New York, N.Y., Pergamon Publishing Co., Chapter 4.

Platt, J. R. (1949), *J. Chem. Phys. 17,* 484.

Pressman, B. C. (1969), *Ann. N. Y. Acad. Sci. 147,* 829.

Pressman, B. C. (1972), *in* The Role of Membranes in Metabolic Regulation, Melman, M. A., and Hanson, R. W., Ed., New York, N.Y., Academic Press.

Pressman, B. C. (1973), *Fed. Proc., Fed. Amer. Soc. Exp. Biol. 32,* 1968.
Pressman, B. C., and Haynes, D. H. (1969), *in* The Molecular Basis of Membrane Function, Testeson, D. C., Ed., Englewood Cliffs, N. J., Prentice-Hall, pp 221–246.
Reichardt, C., and Dimroth, K. (1968), *Fortschr. Chem. Forsch. 11,* 1.
Scarpa, A., and Inesi, G. (1972), *FEBS (Fed. Eur. Biochem. Soc.) Lett. 22,* 273.
Shavit, N., Degani, H. and San-Pietro, A. (1970), *Biochim. Biophys. Acta 216,* 208.
Stark, G., and Benz, R. (1971), *J. Membrane Biol. 5,* 133.
Stevenson, P. E. (1965), *J. Mol. Spectrosc. 15,* 220.
Tinoco, I., Jr. (1962), *Advan. Chem. Phys. 2,* 113–160.
Velluz, L., Legrand, M., and Grosjean, M. (1963), *C. R. Acad. Sci. 256,* 1878.
Wipf, H. K., Pioda, L. A. R., Stefanac, Z., and Simon, W. (1968), *Helv. Chim. Acta 51,* 377.
Yoe, J. H., and Jones, A. L. (1944), *Ind. Eng. Chem., Anal. Ed. 16,* 111.

Role of the Ca^{2+} Concentration Gradient in the Adenosine 5′-Triphosphate–Inorganic Phosphate Exchange Catalyzed by Sarcoplasmic Reticulum†

Leopoldo de Meis* and Maria da Glória Costa Carvalho‡

ABSTRACT: Sarcoplasmic reticulum vesicles isolated from rabbit skeletal muscle catalyze a Ca^{2+}-dependent exchange between orthophosphate and the γ-phosphate of ATP. This exchange occurs both in the presence and in the absence of a transmembrane Ca^{2+} gradient. The exchange catalyzed by solubilized or leaky sarcoplasmic reticulum vesicles is activated by ADP, Ca^{2+} (K_m = 1.6–2.4 mM), and orthophosphate (K_m = 38 mM). In contrast, when a Ca^{2+} concentration gradient is formed across the membrane of intact vesicles, the K_m of orthophosphate is only 3.2 mM. The Ca^{2+} concentration required for half-maximal activation of the ATP $\rightleftharpoons$ P_i exchange reaction is 10^3–2×10^4 times higher than that required for half-maximal activation of Ca^{2+} transport and Ca^{2+}-dependent ATP hydrolysis. In the presence of 8 mM Ca^{2+}, the ATPase activity of leaky or solubilized vesicles is 20–150 times higher than that of ATP $\rightleftharpoons$ P_i exchange.

A highly efficient ATP-dependent system for Ca^{2+} transport has been described in SRV[1] isolated from skeletal muscle (Hasselbach, 1964). In the process of ATP hydrolysis the γ-phosphate of ATP is covalently bound to a membrane protein (E). This phosphoprotein (E–P) represents an intermediary product in the sequence of reactions leading to Ca^{2+} transport and P_i liberation (Yamamoto and Tonomura, 1967; Makinose, 1969; de Meis, 1972). The following sequence has therefore been proposed.

$$\text{ATP} + \text{E} \underset{Mg^{2+}}{\overset{Ca^{2+}}{\rightleftharpoons}} \text{E}-\text{P} + \text{ADP} \quad (1)$$

$$\text{E}-\text{P} \overset{Mg^{2+}}{\rightleftharpoons} \text{E} + \text{P}_i \quad (2)$$

Recently it has been shown that these two reactions can be reversed, *i.e.*, that the Ca^{2+} pump of the SRV is reversible (Barlogie *et al.*, 1971; Makinose, 1971, 1972, 1973; Makinose and Hasselbach, 1971; Hasselbach *et al.*, 1972; Panet and Selinger, 1972; Deamer and Baskin, 1972; Masuda and de Meis, 1974). The following data support this finding.

(*a*) *NET Synthesis of ATP.* When SRV previously loaded with calcium phosphate are incubated in a medium containing ADP, Mg^{2+}, and $^{32}P_i$, it is observed that $^{32}P_i$ interacts with the membrane forming E–P, Ca^{2+} is released at a very fast rate, and [γ-$^{32}P_i$]ATP is formed (Barlogie *et al.*, 1971; Makinose, 1972, 1973; Makinose and Hasselbach, 1971).

(*b*) *ATP $\rightleftharpoons$ P_i Exchange.* When SRV are incubated in a medium containing ATP, Mg^{2+}, $^{32}P_i$, and Ca^{2+}, calcium phosphate is accumulated by the vesicles and a Ca^{2+} concentration gradient is built up until a steady state is reached in which a slow Ca^{2+} efflux is balanced by an ATP-driven influx. When this condition is reached, a steady rate of exchange between P_i and the γ-phosphate of ATP is observed. It has been implied that this exchange is the result of the two reactions shown above operating simultaneously forward (ATP hydrolysis) and backward (ATP synthesis from ADP and $^{32}P_i$) (Makinose, 1971; Racker, 1972). If the SRV are made "leaky" by means of phospholipase A or ether, although the transport ATPase remains unimpaired (Makinose, 1971), the Ca^{2+} concentration gradient is abolished and the ATP $\rightleftharpoons$ P_i exchange reaction is arrested. These data lend support to Mitchell's chemiosmotic hypothesis (conversion of osmotic into chemical energy). Accordingly, the energy required for E–P formation, ATP synthe-

† From the Instituto de Biofísica, Universidade Federal do Rio de Janeiro, Centro de Ciências Médicas, Cidade Universitária, Ilha do Fundão, Rio de Janeiro, GB, Brazil. *Received May 23, 1974.* This investigation was supported in part by the Conselho Nacional de Pesquisas, Brazil (T.C. 16.903 and 17.117), by the Conselho de Ensino para Graduados da U.F.R.J., and by the Banco Nacional de Desenvolvimento Econômico (FUNTEC 241).

‡ Recipient of a fellowship from the Conselho Nacional de Pesquisas, Brazil.

[1] Abbreviations used are: SRV, sarcoplasmic reticulum vesicles; EGTA, ethylene glycol bis(β-aminoethyl ether)-*N,N′*-tetraacetic acid.